The Astrophysical Journal, 835:119 (8pp), 2017 February 1 doi:10.3847/1538-4357/835/2/119

Rosseland and Flux Mean Opacities for Compton Scattering

Juri Poutanen[1,2]
[1] Tuorla Observatory, Department of Physics and Astronomy, University of Turku, Väisäläntie 20, FI-21500 Piikkiö, Finland; juri.poutanen@utu.fi
[2] Nordita, KTH Royal Institute of Technology and Stockholm University, Roslagstullsbacken 23, SE-10691 Stockholm, Sweden
Received 2016 June 30; revised 2016 December 13; accepted 2016 December 14; published 2017 January 23

Abstract

Rosseland mean opacity plays an important role in theories of stellar evolution and X-ray burst models. In the high-temperature regime, when most of the gas is completely ionized, the opacity is dominated by Compton scattering. Our aim here is to critically evaluate previous works on this subject and to compute the exact Rosseland mean opacity for Compton scattering over a broad range of temperature and electron degeneracy parameter. We use relativistic kinetic equations for Compton scattering and compute the photon mean free path as a function of photon energy by solving the corresponding integral equation in the diffusion limit. As a byproduct we also demonstrate the way to compute photon redistribution functions in the case of degenerate electrons. We then compute the Rosseland mean opacity as a function of temperature and electron degeneracy and present useful approximate expressions. We compare our results to previous calculations and find a significant difference in the low-temperature regime and strong degeneracy. We then proceed to compute the flux mean opacity in both free-streaming and diffusion approximations, and show that the latter is nearly identical to the Rosseland mean opacity. We also provide a simple way to account for the true absorption in evaluating the Rosseland and flux mean opacities.

Key words: dense matter – opacity – radiative transfer – scattering – stars: neutron – X-rays: bursts

1. Introduction

The key role in the description of radiation transport through a medium is played by two average opacities. The first one, known as the Rosseland mean opacity,

$$\kappa_{\rm R} = \int_0^\infty d\nu\ (\partial B_\nu/\partial T) \Big/ \int_0^\infty d\nu\ \kappa_\nu^{-1} (\partial B_\nu/\partial T), \qquad (1)$$

is used in the diffusion approximation (and in radiative equilibrium) to relate the temperature gradient to the radiation flux:

$$\boldsymbol{F} = -\frac{ac}{3\kappa_{\rm R}} \boldsymbol{\nabla} T^4. \qquad (2)$$

The second one, known as the flux mean opacity,

$$\kappa_{\rm F} = \int_0^\infty d\nu\ \kappa_\nu\ F_\nu / F, \qquad (3)$$

relates the bolometric radiation flux to the radiative acceleration (see Mihalas & Mihalas 1984, pp. 360–361):

$$\boldsymbol{g}_{\rm rad} = \frac{\kappa_{\rm F}}{c} \boldsymbol{F}. \qquad (4)$$

The Rosseland mean can be computed a priori once the total—absorption and scattering—opacity as a function of photon frequency κ_ν is known. For the flux mean, we also need to specify the spectral energy distribution given by the flux F_ν. In the diffusion approximation, these two opacities coincide for pure absorption and coherent isotropic scattering.

In the high-temperature regime, when most of the gas is completely ionized, the opacity is dominated by Compton scattering. This situation is not so simple because the scattering is incoherent, induced scattering has to be accounted for, and the effective cross section should be used instead of the total cross section. Furthermore, it is a priori not obvious that the Rosseland mean and the flux mean opacities coincide even in the diffusion approximation. The Rosseland mean for a nondegenerate electron gas was considered by Sampson (1959). It was further extended by Chin (1965) to include the effect of electron degeneracy. This work was affected by an error, which also propagated into textbooks (Chiu 1968; Cox & Giuli 1968; Weiss et al. 2004). The corrected method to compute the Rosseland mean was introduced by Buchler & Yueh (1976), who provide also a comprehensive analysis of the previous results. The numerical results presented in that work were approximated by Paczynski (1983) with a simple analytical expression, which was later used in numerous papers on X-ray bursts. An alternative approximation was given by Weaver et al. (1978). The flux mean opacities in the free-streaming limit have been computed by Pozdnyakov et al. (1983, see also Nagirner & Poutanen 1994, Poutanen & Vurm 2010).

In this paper we recompute the Rosseland and the flux mean opacities for Compton scattering and compare our results to the previous calculations. We also provide new analytical formulae that approximate the numerical results well.

2. Relativistic Kinetic Equation for Compton Scattering

Derivation of the Rosseland mean opacity for Compton scattering is based on solution of the relativistic kinetic equation (RKE) in terms of the photon mean free path as a function of its energy. Interaction between photons and electrons (positrons) via Compton scattering accounting for the induced scattering and fermion degeneracy can be described by the explicitly covariant RKE for photons (Buchler & Yueh 1976; de Groot et al. 1980; Nagirner & Poutanen 1993, 1994):

$$\begin{aligned} \underline{x} \cdot \underline{\nabla} n(\boldsymbol{x}) = & \frac{r_{\rm e}^2}{2} \frac{2}{\lambda_{\rm C}^3} \int \frac{d\boldsymbol{p}}{\gamma} \frac{d\boldsymbol{p}_1}{\gamma_1} \frac{d\boldsymbol{x}_1}{x_1}\ F\ \delta^4(\underline{p}_1 + \underline{x}_1 - \underline{p} - \underline{x}) \\ & \times \{ n(\boldsymbol{x}_1)[1 + n(\boldsymbol{x})][\tilde{n}_-(\boldsymbol{p}_1)(1 - \tilde{n}_-(\boldsymbol{p})) \\ & + \tilde{n}_+(\boldsymbol{p}_1)(1 - \tilde{n}_+(\boldsymbol{p}))] - n(\boldsymbol{x})[1 + n(\boldsymbol{x}_1)] \\ & \times [\tilde{n}_-(\boldsymbol{p})(1 - \tilde{n}_-(\boldsymbol{p}_1)) + \tilde{n}_+(\boldsymbol{p})(1 - \tilde{n}_+(\boldsymbol{p}_1))] \}, \end{aligned} \qquad (5)$$

where $\underline{\nabla} = \{\partial/c\partial t, -\boldsymbol{\nabla}\}$ is the four-gradient, r_e is the classical electron radius, and $\lambda_C = h/m_e c$ is the Compton wavelength. Here we defined the dimensionless photon four-momentum as $\underline{x} = \{x, \boldsymbol{x}\} = x\{1, \hat{\boldsymbol{\omega}}\}$, where $\hat{\boldsymbol{\omega}}$ is the unit vector in the photon propagation direction and $x \equiv h\nu/m_e c^2$ is the photon energy in units of the electron rest mass. The photon distribution is described by the occupation number n. The dimensionless electron/positron four-momentum is $\underline{p} = \{\gamma, \boldsymbol{p}\} = \{\gamma, p\hat{\boldsymbol{\Omega}}\} = \gamma\{1, \beta\hat{\boldsymbol{\Omega}}\}$, where $\hat{\boldsymbol{\Omega}}$ is the unit vector along the electron momentum, γ and $p = \sqrt{\gamma^2 - 1}$ are the electron Lorentz factor and its momentum in units of $m_e c$, and β is the velocity in units of c. The electron/positron distributions are described by the occupation numbers $\tilde{n}_\pm$.

The factor F in Equation (5) is the Klein–Nishina reaction rate (Berestetskii et al. 1982)

$$F = \left(\frac{1}{\xi} - \frac{1}{\xi_1}\right)^2 + 2\left(\frac{1}{\xi} - \frac{1}{\xi_1}\right) + \frac{\xi}{\xi_1} + \frac{\xi_1}{\xi}, \quad (6)$$

and

$$\xi = \underline{p}_1 \cdot \underline{x}_1 = \underline{p} \cdot \underline{x}, \qquad \xi_1 = \underline{p}_1 \cdot \underline{x} = \underline{p} \cdot \underline{x}_1 \quad (7)$$

are the four-products of the corresponding momenta. The second equalities in Equation (7) arise from the four-momentum conservation law represented by the delta function in Equation (5).

The electron/positron distribution under the assumption of thermal equilibrium and isotropy is given by the Fermi–Dirac distribution:

$$\tilde{n}_\pm(\boldsymbol{p}) = \frac{1}{\exp\left(\frac{\gamma - 1}{\Theta} - \eta_\pm\right) + 1}, \quad (8)$$

where $\Theta = kT/m_e c^2$ is the dimensionless temperature and $\eta_\pm$ are the degeneracy parameters for positrons and electrons (the ratio of the Fermi energy minus rest mass to temperature) related via $\eta_- + \eta_+ = -2/\Theta$ (see, e.g., Cox & Giuli 1968; page 302 of Weiss et al. 2004). The electron/positron concentrations are given by the integrals over the momentum space:

$$N_\pm = 4\pi\frac{2}{\lambda_C^3}\int_0^\infty p^2 dp\ \tilde{n}_\pm(\boldsymbol{p}), \quad (9)$$

and the density (not including electrons and positrons created by pair production or radiation) is

$$\rho = (N_- - N_+)\mu_e m_p, \quad (10)$$

where $\mu_e = 2/(1 + X)$ is the mean number of nucleons per free ionization electron and X is the mass fraction of hydrogen. The total number density of electrons and positrons is $N_e = N_- + N_+$.

The form of the RKE (5) can be simplified by defining the redistribution functions (RF) via

$$R_\pm(\boldsymbol{x}_1 \to \boldsymbol{x}) = \frac{3}{16\pi}\frac{2}{\lambda_C^3}\frac{1}{N_\pm}\int\frac{d\boldsymbol{p}}{\gamma}\frac{d\boldsymbol{p}_1}{\gamma_1}\tilde{n}_\pm(\boldsymbol{p}_1) \times [1 - \tilde{n}_\pm(\boldsymbol{p})]F\ \delta^4(\underline{p}_1 + \underline{x}_1 - \underline{p} - \underline{x}). \quad (11)$$

The RFs satisfy the symmetry property

$$R_\pm(\boldsymbol{x} \to \boldsymbol{x}_1)\ e^{-x/\Theta} = R_\pm(\boldsymbol{x}_1 \to \boldsymbol{x})\ e^{-x_1/\Theta}, \quad (12)$$

which follows from its definition (11) and the energy conservation $\gamma_1 = \gamma + x - x_1$, or from the detailed balance condition (see Equation (8.2) in Pomraning 1973).

In the absence of strong magnetic field, the medium is isotropic, therefore the RF depends only on the photon energies and the scattering angle (with μ being its cosine), i.e., we can write $R_\pm(\boldsymbol{x}_1 \to \boldsymbol{x}) = R_\pm(x, x_1, \mu)$. Introducing the total RF as

$$R(x, x_1, \mu) = \frac{N_-}{N_e}R_-(x, x_1, \mu) + \frac{N_+}{N_e}R_+(x, x_1, \mu), \quad (13)$$

the kinetic Equation (5) in a steady state can be recast in a standard form of the radiative transfer equation:

$$\hat{\boldsymbol{\omega}} \cdot \boldsymbol{\nabla}_\tau n(\boldsymbol{x}) = -n(\boldsymbol{x})\frac{1}{x}\int_0^\infty x_1 dx_1 \int d^2\hat{\boldsymbol{\omega}}_1\ R(x_1, x, \mu) \times [1 + n(\boldsymbol{x}_1)] + [1 + n(\boldsymbol{x})]\frac{1}{x} \times \int_0^\infty x_1 dx_1 \int d^2\hat{\boldsymbol{\omega}}_1\ R(x, x_1, \mu)\ n(\boldsymbol{x}_1), \quad (14)$$

where $\boldsymbol{\nabla}_\tau = \boldsymbol{\nabla}/\sigma_T N_e$ is the dimensionless gradient, with σ_T being the Thomson cross section.

3. Photon Mean Free Path

Deep inside stars or thermonuclear burning regions of X-ray bursts, the radiation field is nearly isotropic and the diffusion approximation should be rather accurate. We can therefore express the occupation number as

$$n(\boldsymbol{x}) = b_x - l_x \hat{\boldsymbol{\omega}} \cdot \boldsymbol{\nabla}_\tau b_x, \quad (15)$$

where $b_x = 1/[\exp(x/\Theta) - 1]$ is the occupation number for the Planck distribution and l_x is the mean free path (in units of $1/\sigma_T N_e$) for Compton scattering of a photon of energy x. Substituting expansion (15) into Equation (14), noticing that the zeroth-order terms cancel out, keeping only terms of the first order in $\boldsymbol{\nabla}_\tau b_x$, and using condition (12), we get (Sampson 1959; Buchler & Yueh 1976)

$$\hat{\boldsymbol{\omega}} \cdot \boldsymbol{\nabla}_\tau b_x = \frac{1}{x}\int_0^\infty x_1 dx_1 \int d^2\hat{\boldsymbol{\omega}}_1\ R(x_1, x, \mu) \times \left[l_x \hat{\boldsymbol{\omega}} \cdot \boldsymbol{\nabla}_\tau b_x \left(\frac{1 - e^{-x/\Theta}}{1 - e^{-x_1/\Theta}}\right) - l_{x_1}\hat{\boldsymbol{\omega}}_1 \cdot \boldsymbol{\nabla}_\tau b_{x_1}\left(\frac{e^{x_1/\Theta} - 1}{e^{x/\Theta} - 1}\right)\right]. \quad (16)$$

Simple algebra gives a linear integral equation for the mean free path l_x:

$$1 = \frac{1}{x}\int_0^\infty x_1 dx_1 \int d^2\hat{\boldsymbol{\omega}}_1\ R(x_1, x, \mu)\frac{1 - e^{-x/\Theta}}{1 - e^{-x_1/\Theta}} \times \left[l_x - l_{x_1}\frac{x_1}{x}\frac{\hat{\boldsymbol{\omega}}_1 \cdot \boldsymbol{\nabla}\Theta}{\hat{\boldsymbol{\omega}} \cdot \boldsymbol{\nabla}\Theta}\right]. \quad (17)$$

Choosing the coordinate system so that $\hat{\boldsymbol{\omega}} = (0, 0, 1)$, defining $\hat{\boldsymbol{\omega}}_1 = (\sqrt{1 - \mu^2}\cos\phi, \sqrt{1 - \mu^2}\sin\phi, \mu)$ and

$\nabla\Theta \propto (\sin\theta, 0, \cos\theta)$, the integral over solid angle becomes $\int d\mu \int d\phi$, with only the last term in the square brackets depending on ϕ. The azimuthal integral is then

$$\int_0^{2\pi} d\phi \frac{\hat{\omega}_1 \cdot \nabla\Theta}{\hat{\omega} \cdot \nabla\Theta} = \int_0^{2\pi} d\phi\ (\mu + \sqrt{1-\mu^2}\tan\theta\cos\phi) = 2\pi\mu, \qquad (18)$$

so that the square bracket in Equation (17) can be substituted by $l_x - l_{x_1} x_1 \mu/x$ (Sampson 1959). Equation (17) can be further modified by integrating over the angles of the scattered photon:

$$1 = 4\pi \int_0^\infty \frac{x_1}{x} dx_1 \frac{1 - e^{-x/\Theta}}{1 - e^{-x_1/\Theta}} \times \left[l_x R_0(x_1, x) - l_{x_1} \frac{x_1}{x} R_1(x_1, x) \right], \qquad (19)$$

where we introduced the moments of the RF (Nagirner & Poutanen 1994)

$$R_0(x_1, x) = \frac{1}{2}\int_{-1}^{1} R(x_1, x, \mu) d\mu, \qquad (20)$$

$$R_1(x_1, x) = \frac{1}{2}\int_{-1}^{1} R(x_1, x, \mu)\ \mu\ d\mu. \qquad (21)$$

The method for computing these functions is described in the Appendix.

At low temperatures the RFs are extremely peaked at $x_1 \approx x$ and therefore two approximations are often made (Sampson 1959; Buchler & Yueh 1976):

$$l_{x_1} \approx l_x, \qquad (22)$$

$$\frac{1 - e^{-x/\Theta}}{1 - e^{-x_1/\Theta}} \approx 1. \qquad (23)$$

The first approximation is equivalent to the on-the-spot approximation in the theory of radiative transfer in spectral lines. These approximations reduce Equation (19) for the mean free path to

$$\frac{1}{l_x} \approx s_0(x) - s_1(x), \qquad (24)$$

where (Nagirner & Poutanen 1994)

$$s_i(x) = \frac{4\pi}{x^{i+1}} \int x_1^{i+1} dx_1 R_i(x_1, x), \quad i = 0, 1. \qquad (25)$$

At temperatures above 50 keV, approximation (23) fails (see Figure 1). Still keeping the on-the-spot approximation (22), we get an explicit expression

$$\frac{1}{l_x} \approx r_0(x) - r_1(x), \qquad (26)$$

where

$$r_i(x) = \frac{4\pi}{x^{i+1}} \int x_1^{i+1} dx_1 R_i(x_1, x) \frac{1 - e^{-x/\Theta}}{1 - e^{-x_1/\Theta}}. \qquad (27)$$

At low temperatures, the easiest way to exactly solve Equation (19) for l_x is to use an iteration procedure, starting from the approximation (26). The functions $r_i(x)$ can be

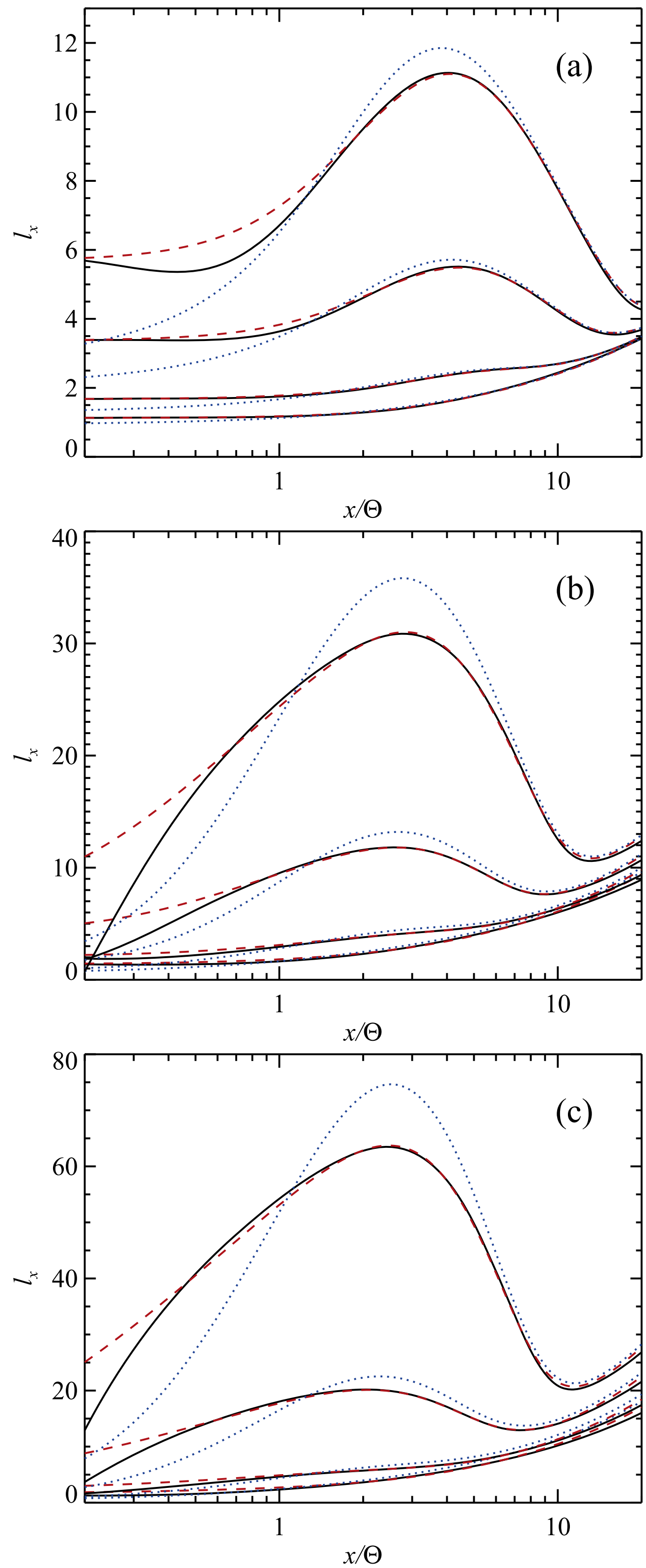

Figure 1. Mean free path of photons l_x (in units of $1/\sigma_T N_e$) as a function of the ratio of photon energy to temperature for various temperatures and degeneracies: (a) $\Theta = 0.05$, (b) $\Theta = 0.25$, (c) $\Theta = 0.5$. Different lines from bottom to top correspond to the degeneracy parameter $\eta = -2, 1, 4, 7$. The exact solution (19) is shown by the solid black lines. The approximate expressions (24) and (26) are shown by the dotted blue and dashed red lines, respectively.

tabulated in advance. The integrals over the energy x_1 for every x have to be taken over a dense grid around x. For high temperatures, in principle, one can replace the integral by the discrete sum on a logarithmic grid of photon energies x_i and solve Equation (19) as a system of linear equations for $l_i = l_{x_i}$ (as was done by Buchler & Yueh 1976):

$$\frac{1}{4\pi} = l_i\, a_i + \sum_j l_j\, b_{ij} = \sum_j l_j\, (b_{ij} + a_i \delta_{ij}), \qquad (28)$$

where

$$a_i = \sum_j w_j \frac{x_j}{x_i} \frac{1 - e^{-x_i/\Theta}}{1 - e^{-x_j/\Theta}} R_0(x_j, x_i), \qquad (29)$$

$$b_{ij} = -w_j \frac{x_j^2}{x_i^2} \frac{1 - e^{-x_i/\Theta}}{1 - e^{-x_j/\Theta}} R_1(x_j, x_i), \qquad (30)$$

and w_j are the integration weights (equal to $x_j\, \Delta \ln x$ for a logarithmic grid) and δ_{ij} is the Kronecker delta. The results of calculations for l_x using a solution of the integral equation as well as by approximate formulae (26) and (24) are presented in Figure 1.

We see that the mean free path computed using expression (26) approximates the exact l_x well at all photon energies x for low temperature and small degeneracy parameter η as well as at $x \gtrsim \Theta$ for large Θ and η. The approximate expression (24) used by Sampson (1959) is also reasonably accurate for small Θ and η for $x \gtrsim \Theta$, but becomes increasingly inaccurate for high Θ and η. We note that for large Θ and η the solution of the integral Equation (19) gives negative l_x at small x, which is unphysical; on the other hand, l_x computed via Equation (26) is always positive.

4. Rosseland Mean Opacity

After finding the mean free path l_x as a solution of Equation (19), we can compute the Rosseland mean opacity as

$$\kappa_{\rm R} = \frac{\sigma_{\rm T} N_{\rm e}}{\rho} \frac{1}{\Lambda}, \qquad (31)$$

where the Rosseland mean free path (in units of $1/\sigma_{\rm T} N_{\rm e}$) is

$$\Lambda(\Theta, \eta_-) = \frac{\int_0^\infty l_x \frac{\partial B_x}{\partial \Theta} dx}{\int_0^\infty \frac{\partial B_x}{\partial \Theta} dx} = \frac{15}{4\pi^4} \int_0^\infty l_x \frac{u^4 e^u}{(e^u - 1)^2} du, \qquad (32)$$

and $u = x/\Theta = h\nu/kT$ and $B_x = x^3 b_x$. The integrals over x are taken over the energy range where l_x is positive. We note that because of the high accuracy of the approximation (26), the Rosseland mean can also be computed using an explicit expression instead of solving integral Equation (19), typically giving a relative accuracy of better than 10^{-4}. This approximation also allows us to easily find the photon mean free path when, additionally, true absorption needs to be accounted for: $1/l_x \approx \alpha(x) + r_0(x) - r_1(x)$, where $\alpha(x)$ is the standard absorption coefficient in units of $\sigma_{\rm T} N_{\rm e}$.

The results of calculations for Λ over a broad range of temperatures and electron degeneracies η_- are presented in Figures 2 and 3. We present the results taking opacity by electrons only, as was done also by Sampson (1959) and Buchler & Yueh (1976), because there are no pairs at low temperatures or high degeneracies. At low degeneracies and high temperatures $\Theta > -1/\eta$; on the other hand, the number of positrons exceeds the number of electrons, because $\eta_+ = -2/\Theta - \eta_- > \eta_-$, which is unphysical. In the following we will replace η_- by η. The results computed by Sampson (1959) and Buchler & Yueh (1976) are shown by triangles and circles, respectively, while our results are shown by black solid curves. The results of Sampson (1959) are accurate to better than 1% up to about 25 keV; after that they start to deviate significantly. This is a direct consequence of his usage of approximation (24) for the mean free path, which is supported by our calculations in the same approximation (see dotted blue curves in Figures 2 and 3(b), and the residuals in the bottom panel of Figure 2). We see that this approximation systematically underestimates the opacity at high temperatures. We note here that the opacity computed by Chin (1965) for degenerate electrons and still reprinted in the textbooks (Weiss et al. 2004) is systematically too large by up to 13% (see black squares in Figure 3(a)); a rather good agreement at high temperatures results from a fortuitous cancellation of an error and his usage of approximation (24) (Buchler & Yueh 1976).

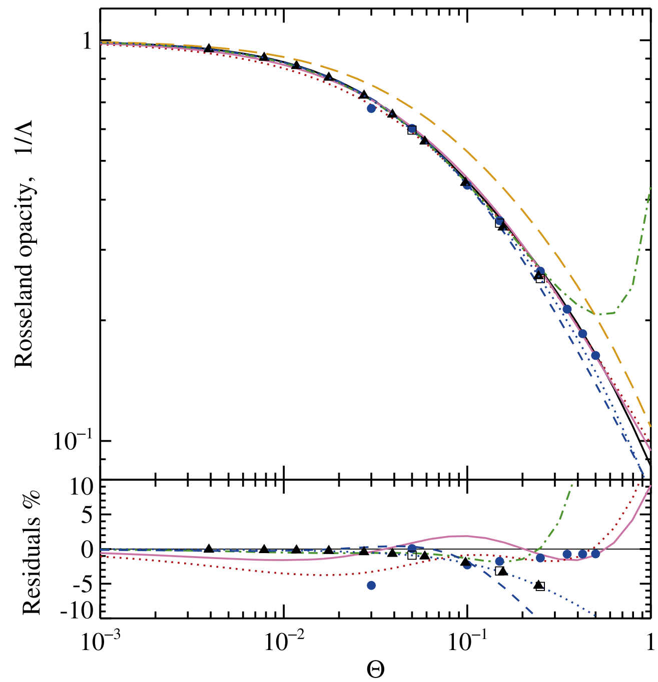

Figure 2. Rosseland mean opacity (in units of $\sigma_{\rm T} N_{\rm e}/\rho$) as a function temperature for nondegenerate gas. The black solid curve represents the result of our exact calculations. The dotted blue curves give the Rosseland mean computed with the help of approximation (24) for the mean free path. The blue circles give the numerical results of Buchler & Yueh (1976), the black triangles are the results from Sampson (1959), and the open squares are from Chin (1965). The dotted red curve is the Paczyński approximation (35), which underestimates exact results by 2%–3%. The solid pink curve is the best fit in the temperature range 2–300 keV using function (41) with parameters $T_0 = 41.5$ keV and $\alpha_0 = 0.9$, which is accurate to within 2% in that range. The dashed blue curve is the same approximation in the temperature range 2–40 keV with parameters $T_0 = 39.4$ keV and $\alpha_0 = 0.976$, which is accurate to 0.7%. The dot-dashed green curve is the approximation (33), which is accurate to within 3% in the temperature range 1–150 keV and rapidly diverges at higher temperatures. The long-dashed brown curve represents the flux mean opacity in the free-streaming limit (49) for the blackbody spectrum. The bottom panel presents the residuals as a percentage of our exact calculations.

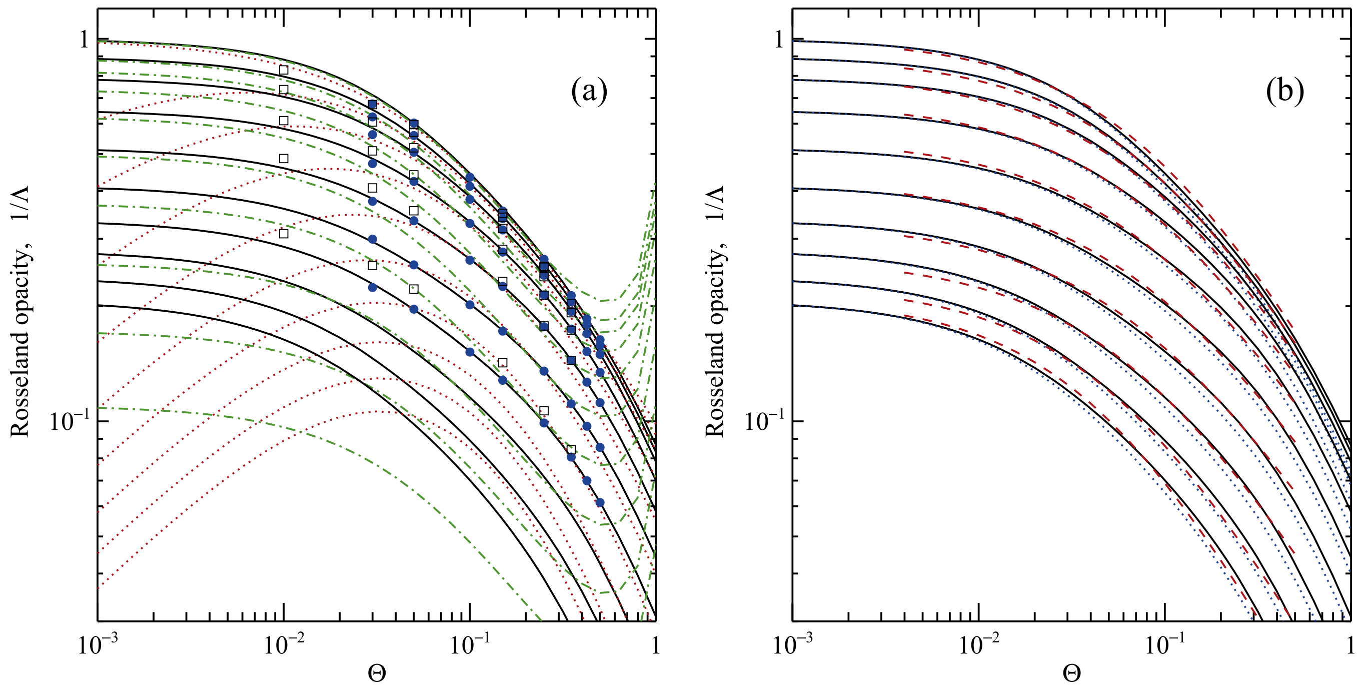

Figure 3. Rosseland mean opacity (in units of $\sigma_T N_e/\rho$) as a function of temperature for various values of the degeneracy parameter η. The solid black curves represent the result of our exact calculations (the flux mean opacity is equal to the Rosseland mean to within 10^{-4}). The top curve corresponds to $\eta = -10$; for the following curves η varies from −1 to 7. (a) The blue circles give the numerical results of Buchler & Yueh (1976) for $\eta = -10, -1, .., 4$ and the black open squares are from Chin (1965) for $\eta = -\infty, -1, 0, 1, 2, 4$ (for five values of Θ, except for $\eta = -\infty$ for which the opacity is given for only three, $\Theta = 0.05, 0.15, 0.25$). The dot-dashed green curves are the approximation (33) and dotted red curves give Paczyński's approximation (35). (b) The dotted blue curves are the Rosseland mean computed using approximation (24) for the mean free path and the dashed red curves correspond to our approximate expression (36) for the range 2–300 keV.

On the other hand, the results of Buchler & Yueh (1976) are within 2% of ours above 25 keV ($\Theta > 0.05$), but at $\Theta = 0.03$ they underestimate the opacity by as much as 6%. The situation becomes worse if we use the analytical approximations of Buchler & Yueh (1976) at lower temperatures, where the opacity would be systematically underestimated by up to 13%.

The calculations of Buchler & Yueh (1976) gave rise to at least two different approximate formulae for the Rosseland mean opacity. Weaver et al. (1978) separated the dependences on Θ and η:

$$\Lambda_{W78}(\Theta, \eta) = f_\Theta f_\eta, \tag{33}$$

where

$$f_\Theta = 1 + 14.1\Theta - 12.7\Theta^2 \quad (\text{for } \Theta < 0.4),$$
$$f_\eta = 1 + \exp(0.522\eta - 1.563). \tag{34}$$

Expressions (33) and (34) were claimed to be accurate to better than 10% over a wide range of degeneracy parameters and temperatures ($-\infty < \eta \lesssim 4$, $0.04 < \Theta < 0.4$). This approximation is used in the codes developed for simulation of stellar evolution and explosions, including X-ray bursts (Woosley et al. 2002, 2004). We see (Figure 3(a)) that it diverges above 150 keV for any η. Because the dependences on T and η are separated, the temperature range of applicability of this approximation becomes smaller for large η. For $\eta = 4$ deviations from the exact values reach 50% in the middle of the temperature range where the approximation is supposed to work.

A different approximation that is widely used in theory of X-ray bursts was given by Paczynski (1983):

$$\Lambda_{P83}(\Theta, \eta) = \left[1 + \left(\frac{kT}{38.8\ \text{keV}}\right)^{0.86}\right][1 + 2.7 \times 10^{11}\ \rho T^{-2}] \tag{35}$$

for $\mu_e = 2$. We see from Figures 2 and 3(a) that Paczyński's approximation is rather good for small η. At large η it becomes highly inaccurate at low temperatures.

For the approximation of the Rosseland mean opacity, we propose to use a combination of the forms proposed by Buchler & Yueh (1976) and Paczynski (1983):

$$\Lambda_{app}(\Theta, \eta) = f_1(\eta)[1 + (T/T_{br})^\alpha], \tag{36}$$

where

$$T_{br} = T_0 f_2(\eta), \tag{37}$$

$$\alpha = \alpha_0 f_3(\eta), \tag{38}$$

$$f_i(\eta) = 1 + c_{i1}\xi + c_{i2}\xi^2, \quad i = 1, 2, 3, \tag{39}$$

$$\xi = \exp(c_{01}\eta + c_{02}\eta^2). \tag{40}$$

The coefficients are given in Table 1 for two fitting intervals 2–40 and 2–300 keV. This form approximates the opacity to better than 4% and 6.5% over the whole range of degeneracy parameter $-10, \ldots, 7$ in the temperature ranges 2–40 and 2–300 keV, respectively (see Figure 3(b)). In case of a nondegenerate gas, $\eta \to -\infty$, the expressions simplify

Table 1
Coefficients of the Approximate Formulae (41) and (36)

Coefficient	Rosseland Mean				Flux Mean[a]
	2–40 keV		2–300 keV		2–300 keV
T_0	39.4	43.4	41.5	43.3	58.5
α_0	0.976	0.902	0.90	0.885	0.913
c_{01}	⋯	0.777	⋯	0.682	⋯
c_{02}	⋯	−0.0509	⋯	−0.0454	⋯
c_{11}	⋯	0.25	⋯	0.24	⋯
c_{12}	⋯	−0.0045	⋯	0.0043	⋯
c_{21}	⋯	0.0264	⋯	0.050	⋯
c_{22}	⋯	−0.0033	⋯	−0.0067	⋯
c_{31}	⋯	0.0046	⋯	−0.037	⋯
c_{32}	⋯	−0.0009	⋯	0.0031	⋯

Note.
[a] The flux mean opacity in the free-streaming limit for a blackbody spectrum of the same temperature as given by Equation (49).

because all $f_i = 1$:

$$\Lambda_{\rm app}(\Theta) = 1 + (T/T_0)^{\alpha_0}, \quad (41)$$

with the best-fit parameters given in Table 1. The goodness of the fits is demonstrated in Figure 2. We note, however, that physically realistic parameters should correspond to $N_- > N_+$, which demands $\Theta < -1/\eta$, i.e., for $\eta = -10$ the temperature is limited to 50 keV.

5. Radiative Acceleration and the Flux Mean Opacity

Radiative acceleration of the medium can be given by the product of the flux and the flux mean opacity. As we mentioned in the Introduction, the flux mean is identical (in the diffusion approximation) to the Rosseland mean only in the case of pure absorption and coherent isotropic scattering. These conditions are not satisfied in case of Compton scattering. Obviously, in the optically thin limit the flux mean depends on the photon spectral energy distribution and cannot be determined a priori. In this section, we derive expressions for the flux mean opacities in both the free-streaming and diffusion limits.

To compute the radiation force on the medium, we need to construct the first moment of the RKE. Multiplying RKE (14) by $\boldsymbol{x}$ and integrating over $d\boldsymbol{x}$, we get

$$-\boldsymbol{\nabla}_\tau\cdot\mathsf{T} = \int\frac{d\boldsymbol{x}}{x}\int\frac{d\boldsymbol{x}_1}{x_1}R(x_1, x, \mu)n(\boldsymbol{x})[1+n(\boldsymbol{x}_1)](\boldsymbol{x}-\boldsymbol{x}_1), \quad (42)$$

where we changed the variables $\boldsymbol{x} \leftrightarrow \boldsymbol{x}_1$ in the second half of the equation and introduced the (dimensionless) radiation pressure tensor

$$\mathsf{T} = \int \boldsymbol{x}\boldsymbol{x}n(\boldsymbol{x})\ \frac{d\boldsymbol{x}}{x}. \quad (43)$$

This tensor is related to the ordinary radiation pressure tensor by

$$\mathsf{P} = 2\frac{m_{\rm e}c^2}{\lambda_{\rm C}^3}\mathsf{T}. \quad (44)$$

Let us represent the gradient of the pressure tensor as a sum of the terms that are linear and quadratic in n:

$$\boldsymbol{\nabla}_\tau\cdot\mathsf{T} = \boldsymbol{\nabla}_\tau\cdot\mathsf{T}_0 + \boldsymbol{\nabla}_\tau\cdot\mathsf{T}_{\rm l}. \quad (45)$$

Integrating over angles $d^2\omega_1$, the first term becomes

$$-\boldsymbol{\nabla}_\tau\cdot\mathsf{T}_0 = \int\frac{d\boldsymbol{x}}{x}\ n(\boldsymbol{x})\ 4\pi\hat{\boldsymbol{\omega}}\int_0^\infty x_1\,dx_1\,[xR_0(x_1, x) - x_1R_1(x_1, x)] = 4\pi\int x^3dx\ \boldsymbol{h}_x[s_0(x) - s_1(x)], \quad (46)$$

where

$$\boldsymbol{h}_x = \frac{1}{4\pi}\int\ \hat{\boldsymbol{\omega}}n(\boldsymbol{x})\ d\hat{\boldsymbol{\omega}} \quad (47)$$

is the first moment of n and $x[s_0(x) - s_1(x)]N_{\rm e}\sigma_{\rm T}m_{\rm e}c$ is the momentum transfer per unit length of photon propagation averaged over electron distribution and scattered photon directions ignoring induced scattering (Nagirner & Poutanen 1994; Poutanen & Vurm 2010; Pozdnyakov et al. 1983). Note that the radiation flux in these notations is

$$\boldsymbol{F} \propto \int x^3dx\ \boldsymbol{h}_x. \quad (48)$$

Thus the flux mean opacity (in units of $N_{\rm e}\sigma_{\rm T}/\rho$) in the free-streaming limit (ignoring induced scattering) is

$$\kappa_{\rm F} = \frac{\int x^3dx\ h_x\ [s_0(x) - s_1(x)]}{\int x^3dx\ h_x}. \quad (49)$$

For the radiation spectrum close to a diluted blackbody, i.e., $h_x \propto b_x$, the flux mean opacity for the case of nondegenerate electrons is shown in Figure 2. It can be approximated by Equation (41) with parameters $T_0 = 58.5$ keV and $\alpha_0 = 0.913$ to better than 0.8% accuracy in the range 2–300 keV. On the other hand, a nonrelativistic approximation (2.63) from Pozdnyakov et al. (1983), $\kappa_{\rm F} = 1 - 10.26\Theta$, fails already above 5 keV.

In the diffusion approximation (15), we substitute $\boldsymbol{h}_x = -\frac{1}{3}l_x\boldsymbol{\nabla}_\tau b_x$. The effect of the induced scattering on the radiation pressure force in the diffusion approximation can be computed by substituting Equation (15) into Equation (42). The nonlinear term becomes

$$-\boldsymbol{\nabla}_\tau\cdot\mathsf{T}_{\rm l} = \int xdx\int x_1dx_1\int d^2\omega\int d^2\omega_1(b_x + \eta l_x\partial_\tau b_x) \times (b_{x_1} + \eta_1 l_{x_1}\partial_\tau b_{x_1})R(x_1, x, \mu)(x\hat{\boldsymbol{\omega}} - x_1\hat{\boldsymbol{\omega}}_1), \quad (50)$$

where $\hat{\boldsymbol{\omega}} = (\sqrt{1-\eta^2}\cos\phi, \sqrt{1-\eta^2}\sin\phi, \eta)$ and $\hat{\boldsymbol{\omega}}_1 = (\sqrt{1-\eta_1^2}\cos\phi_1, \sqrt{1-\eta_1^2}\sin\phi_1, \eta_1)$ with the z-axis chosen against the temperature gradient and $\partial_\tau b_x \equiv |\boldsymbol{\nabla}_\tau b_x|$. Taking the angular integrals, for the magnitude of the radiation pressure force we get

$$-|\boldsymbol{\nabla}_\tau\cdot\mathsf{T}_{\rm l}| = \frac{16\pi^2}{3}\int xdx\int x_1dx_1[R_0(x_1, x) \times (b_{x_1}xl_x\partial_\tau b_x - b_xx_1l_{x_1}\partial_\tau b_{x_1}) + R_1(x_1, x) \times (xb_xl_{x_1}\partial_\tau b_{x_1} - x_1b_{x_1}l_x\partial_\tau b_x)]. \quad (51)$$

Making the change of variables $x \leftrightarrow x_1$ in the terms containing $\partial_\tau b_{x_1}$, we get

$$-|\nabla_\tau \cdot \mathsf{T}_1| = \frac{16\pi^2}{3} \int x dx\ l_x \partial_\tau b_x \int x_1 dx_1 b_{x_1} \{ [xR_0(x_1, x) - x_1 R_1(x_1, x)] - [xR_0(x, x_1) - x_1 R_1(x, x_1)] \}. \tag{52}$$

The total pressure gradient becomes

$$\begin{aligned} -|\nabla_\tau \cdot \mathsf{T}| &= \frac{16\pi^2}{3} \int x dx\ l_x \partial_\tau b_x \int x_1 dx_1 \{ (1 + b_{x_1}) \\ &\times [xR_0(x_1, x) - x_1 R_1(x_1, x)] \\ &- b_{x_1} [xR_0(x, x_1) - x_1 R_1(x, x_1)] \} \\ &= \frac{16\pi^2}{3} \int x dx\ l_x \partial_\tau b_x \int x_1 dx_1 \frac{1 - e^{-x/\Theta}}{1 - e^{-x_1/\Theta}} \\ &\times [xR_0(x_1, x) - x_1 R_1(x_1, x)] \\ &= \frac{4\pi}{3} \int x^3 dx\ l_x \partial_\tau b_x [r_0(x) - r_1(x)]. \end{aligned} \tag{53}$$

Thus the flux mean opacity is then

$$\kappa_{\rm F} = \frac{\int_0^\infty l_x\ [r_0(x) - r_1(x)] \frac{\partial B_x}{\partial \Theta} dx}{\int_0^\infty l_x \frac{\partial B_x}{\partial \Theta} dx}. \tag{54}$$

Because approximation (26), i.e., $1/l_x \approx r_0(x) - r_1(x)$, is very accurate in the region of the photon energies $x \sim \Theta$ contributing to the integral, the flux mean opacity in the diffusion approximation turned out to be nearly identical (but not equal: the relative difference is less than 10^{-4}) to the Rosseland mean over the full range of temperatures and degeneracies considered. The flux mean opacity can thus be approximated by simple analytical expressions (36) and (41), which also describe well the radiative acceleration in the atmospheres of hot neutron stars obtained from the solution of the radiative transfer equation with the exact Compton redistribution function where the diffusion approximation has not been used (Suleimanov et al. 2012).

6. Summary

In this paper, we have critically evaluated the results of previous works on the Rosseland mean opacity for Compton scattering. In order to obtain the photon mean free path as a function of photon energy we have solved in the diffusion approximation the relativistic kinetic equation describing photon interactions via Compton scattering with the possibly degenerate electron gas. We demonstrated that the mean free path can be also accurately evaluated using explicit approximate formulae, which can also be used for calculations of the Rosseland mean opacity and can provide a simple way to account for the true absorption.

We have computed the Rosseland mean opacity over a broad range of temperature and electron degeneracy parameter. We compared our results to previous calculations and found a significant difference in the low-temperature regime. We have also presented useful analytical expressions that approximate the numerical results well. We then computed the flux mean opacities in the free-streaming limit as well as in the diffusion approximation, finding that the latter is nearly identical to the Rosseland mean opacity.

The author thanks Valery Suleimanov, Dmitri Nagirner, and Dmitry Yakovlev for useful discussions. This work was supported by the Foundations' Professor Pool, the Finnish Cultural Foundation, and the Academy of Finland grant 268740. The author also acknowledges useful conversations with the members of the X-ray burst team of the International Space Science Institute (Bern, Switzerland).

Appendix
Redistribution Functions

The RF defined by Equation (11) has been studied in detail before in the case of nondegenerate electrons (Aharonian & Atoyan 1981; Prasad et al. 1986; Nagirner & Poutanen 1994; Poutanen & Vurm 2010). This RF can be simplified to the one-dimensional integral over the electron energy. It turned out that the derivation is identical for degenerate electrons, and also in this case the RF can be presented in terms of one integral that can be taken numerically.

For the isotropic electron distribution, expression (11) for the RF can be simplified by taking the integral over $\boldsymbol{p}$ with the help of the three-dimensional delta function and using the identity $\delta(\gamma_1 + x_1 - \gamma - x) = \gamma\delta(\underline{x}_1 \cdot \underline{p}_1 - \underline{x} \cdot (\underline{p}_1 + \underline{x}_1))$:

$$R_\pm(x, x_1, \mu) = \frac{3}{16\pi} \frac{2}{\lambda_{\rm C}^3 N_\pm} \int \frac{d\boldsymbol{p}_1}{\gamma_1} \tilde{n}_\pm(\gamma_1)[1 - \tilde{n}_\pm(\gamma)] F\delta(\Gamma), \tag{55}$$

where

$$\gamma = \gamma_1 + x_1 - x, \tag{56}$$

$$\Gamma = \gamma_1(x_1 - x) - p_1(x_1\hat{\boldsymbol{\omega}}_1 - x\hat{\boldsymbol{\omega}}) \cdot \hat{\boldsymbol{\Omega}}_1 - q, \tag{57}$$

$$q = \boldsymbol{x} \cdot \boldsymbol{x}_1 = xx_1(1 - \mu). \tag{58}$$

The RF also depends implicitly on the electron temperature Θ and degeneracy parameter $\eta_\pm$. To integrate over angles in Equation (A1) we follow the recipe proposed by Aharonian & Atoyan (1981) (see also Prasad et al. 1986; Poutanen & Vurm 2010), choosing the polar axis along the direction of the transferred momentum

$$\hat{\boldsymbol{n}} \equiv (x_1\hat{\boldsymbol{\omega}}_1 - x\hat{\boldsymbol{\omega}})/Q, \tag{59}$$

where

$$Q^2 = (x_1\hat{\boldsymbol{\omega}}_1 - x\hat{\boldsymbol{\omega}})^2 = (x - x_1)^2 + 2q. \tag{60}$$

Thus the integration variables become $\cos\alpha = \hat{\boldsymbol{n}} \cdot \hat{\boldsymbol{\Omega}}_1$ and the corresponding azimuth Φ. The RF (55) then can be written as

$$R_\pm(x, x_1, \mu) = \frac{3}{16\ \pi} \frac{2}{\lambda_{\rm C}^3 N_\pm} \int_1^\infty \tilde{n}_\pm(\gamma_1)[1 - \tilde{n}_\pm(\gamma)] p_1 d\gamma_1 \times \int_{-1}^1 \delta(\Gamma)\ d\cos\alpha \int_0^{2\pi} F d\Phi, \tag{61}$$

where now

$$\Gamma = \gamma_1(x_1 - x) - q - p_1 Q \cos\alpha. \tag{62}$$

Integrating over $\cos\alpha$ using the delta function, we get

$$R_\pm(x, x_1, \mu) = \frac{3}{8} \frac{2}{\lambda_{\rm C}^3 N_\pm} \int_{\gamma_*}^\infty \tilde{n}_\pm(\gamma_1) \times [1 - \tilde{n}_\pm(\gamma)]\ R(x, x_1, \mu, \gamma_1)\ d\gamma_1, \tag{63}$$

with integration over the electron distribution done numerically. Here we introduced the RF for monoenergetic electrons

$$R(x, x_1, \mu, \gamma_1) = \frac{1}{Q}\frac{1}{2\pi}\int_0^{2\pi} F\, d\Phi. \quad (64)$$

The function F depends on $\xi_1 = x(\gamma_1 - p_1\zeta)$ and $\xi = \xi_1 + q$, where

$$\zeta = \hat{\boldsymbol{\omega}}\cdot\hat{\boldsymbol{\Omega}}_1 = \cos\alpha\cos\kappa + \sin\alpha\sin\kappa\cos\Phi, \quad (65)$$

$$\cos\alpha = \hat{\boldsymbol{n}}\cdot\hat{\boldsymbol{\Omega}}_1 = [\gamma_1(x_1 - x) - q]/p_1 Q, \quad (66)$$

$$\cos\kappa = \hat{\boldsymbol{\omega}}\cdot\hat{\boldsymbol{n}} = (x_1\mu - x)/Q. \quad (67)$$

The condition $|\cos\alpha| \leqslant 1$, gives a constraint

$$\gamma_1 \geqslant \gamma_*(x, x_1, \mu) = (x - x_1 + Q\sqrt{1 + 2/q})/2. \quad (68)$$

Integrating over azimuth Φ in Equation (64) gives the exact analytical expression for the RF valid for any photon and electron energy (Buchler & Yueh 1976; Aharonian & Atoyan 1981; Prasad et al. 1986; Nagirner & Poutanen 1994; Poutanen & Vurm 2010), which we use in our calculations:

$$R(x, x_1, \mu, \gamma_1) = \frac{2}{Q} + \frac{q^2 - 2q - 2}{q^2}\left(\frac{1}{a_-} - \frac{1}{a_+}\right) + \frac{1}{q^2}\left(\frac{d_-}{a_-^3} + \frac{d_+}{a_+^3}\right), \quad (69)$$

where

$$a_-^2 = (\gamma_1 - x)^2 + \frac{1+\mu}{1-\mu}, \quad a_+^2 = (\gamma_1 + x_1)^2 + \frac{1+\mu}{1-\mu},$$
$$d_\pm = (a_+^2 - a_-^2 \pm Q^2)/2. \quad (70)$$

The cancellations at small photon energies have been handled by Nagirner & Poutanen (1993). We note that the RF (69) satisfies the detailed balance condition (Nagirner & Poutanen 1994):

$$R(x, x_1, \mu, \gamma_1) = R(x_1, x, \mu, \gamma_1 + x_1 - x). \quad (71)$$

The RF (55) is related to the scattering kernel (8.13) in Pomraning (1973) by $R(x, x_1, \mu) = \sigma_s(x_1 \to x, \mu)x_1/x$. The form given by Equation (61) is equivalent to Equation (A4) in Buchler & Yueh (1976). The derived RF for monoenergetic electrons (69) is equivalent to Equation (A5) from Buchler & Yueh (1976) and Equation (14) in Aharonian & Atoyan (1981).

The angle-averaged RF functions (20) and (21), used in the calculations of the mean free path, can be expressed through the single integral over the electron and positron distributions

$$R_i(x, x_1) = \frac{3}{16}\frac{2}{\lambda_C^3 N_e}\int_{\gamma'_\star}^{\infty} R_i(x, x_1, \gamma_1)\, d\gamma_1 \{\tilde{n}_-(\gamma_1)[1 - \tilde{n}_-(\gamma)] + \tilde{n}_+(\gamma_1)[1 - \tilde{n}_+(\gamma)]\}, \quad i = 0, 1, \quad (72)$$

where

$$\gamma'_\star(x, x_1) = \begin{cases} \frac{x - x_1}{2} + \frac{x + x_1}{2}\sqrt{1 + \frac{1}{xx_1}} & \text{if } |x - x_1| \geqslant 2xx_1, \\ 1 + (x - x_1 + |x - x_1|)/2 & \text{if } |x - x_1| \leqslant 2xx_1. \end{cases} \quad (73)$$

The explicit analytical expressions for the angle-integrated functions $R_0(x, x_1, \gamma_1)$ and $R_0 - R_1$ under the integral in Equation (72) can be found in Sections 8.1 and 8.2 of Nagirner & Poutanen (1994).

References

Aharonian, F. A., & Atoyan, A. M. 1981, Ap&SS, 79, 321
Berestetskii, V. B., Lifshitz, E. M., & Pitaevskii, V. B. 1982, Quantum Electrodynamics (Oxford: Pergamon)
Buchler, J. R., & Yueh, W. R. 1976, ApJ, 210, 440
Chin, C.-W. 1965, ApJ, 142, 1481
Chiu, H.-Y. 1968, Stellar Physics, Vol. 1 (Waltham, MA: Blaisdell)
Cox, J. P., & Giuli, R. T. 1968, Principles of Stellar Structure (New York: Gordon and Breach)
de Groot, S. R., van Leeuwen, W. A., & van Weert, C. G. 1980, Relativistic Kinetic Equation (Amsterdam: North-Holland)
Mihalas, D., & Mihalas, B. W. 1984, Foundations of Radiation Hydrodynamics (New York: Oxford Univ. Press)
Nagirner, D. I., & Poutanen, J. 1993, A&A, 275, 325
Nagirner, D. I., & Poutanen, J. 1994, ASPRv, 9, 1
Paczynski, B. 1983, ApJ, 267, 315
Pomraning, G. C. 1973, The Equations of Radiation Hydrodynamics (Oxford: Pergamon)
Poutanen, J., & Vurm, I. 2010, ApJS, 189, 286
Pozdnyakov, L. A., Sobol, I. M., & Syunyaev, R. A. 1983, ASPRv, 2, 189
Prasad, M. K., Kershaw, D. S., & Beason, J. D. 1986, ApPhL, 48, 1193
Sampson, D. H. 1959, ApJ, 129, 734
Suleimanov, V., Poutanen, J., & Werner, K. 2012, A&A, 545, A120
Weaver, T. A., Zimmerman, G. B., & Woosley, S. E. 1978, ApJ, 225, 1021
Weiss, A., Hillebrandt, W., Thomas, H.-C., & Ritter, H. 2004, Cox and Giuli's Principles of Stellar Structure (Cambridge: Cambridge Scientific)
Woosley, S. E., Heger, A., Cumming, A., et al. 2004, ApJS, 151, 75
Woosley, S. E., Heger, A., & Weaver, T. A. 2002, RvMP, 74, 1015